X-ray fluorescence, X-ray powder diffraction and Raman spectrosopy

Wubulikasimu Yibulayin, Lovro Pavletić, Kuerbannisa Muhetaer

12.05.2016.

Abstract

In this report we report about the experiments that were made at the School of Science and Technology in Camerino. The experiments performed here are the determinations of unknown samples using X-ray fluorescence (XRF), powder diffraction of bulk and nano Bismuth crystals using X-ray diffraction (XRD), and resolution test of Micro Raman system. We present results of detected elements using qualitative analysis of XRF pattern, as well as the particle sizes of Bi crystals using XRD powder spectra, and a description about the change in the resolution when different grating number and magnification on the Micro Raman setup is used.

Contents

1 Theoretical background **1**
1.1 X-ray flourescence 1
1.2 X-ray powder diffraction 2
1.3 Raman spectroscopy 2

2 XRF of the unknown samples **3**
2.1 Experimental setup 3
2.2 Results and discussion 3

3 Powder diffraction of bulk and nano Bismuth crystal **4**
3.1 Experimental setup 4
3.2 Results and discussion 4

4 Resolution Test of Micro Raman System **5**
4.1 Experimental setup 5
4.2 Results and discussion 5

5 Conclusions **7**

1 Theoretical background

1.1 X-ray flourescence

X-Ray fluorescence technique, also known for its acronym XRF is one of the most widespread and useful methods for the determination of presence and quantity of the elements in a given substance. It is a consequence of the ionization of atoms, for which the excited state returns to the ground state emitting X-ray photons of well-defined energies. The examination of the XRF spectra allows us to identify the atomic species present in a given sample. In fact, the energy of the X-ray emission lines is a well-defined function of the atomic number Z. For its powerful information content and simple application methodology, the XRF technique is applied in many different contexts and fields. An important feature of the XRF is the possibility of performing a chemical analysis in a rapid and non-destructive way. In particular this technique allows us qualitative and quantitative analysis. Qualitative analysis which is used in this report is limited to the identification of the atomic species, and it is relatively simple. Nevertheless, in some cases there is an almost perfect overlap of emission lines of two successive series hindering the identification of some elements. In those cases a better energy resolution of the detector (obtained for example using an angular dispersion technique) may be necessary.[1]

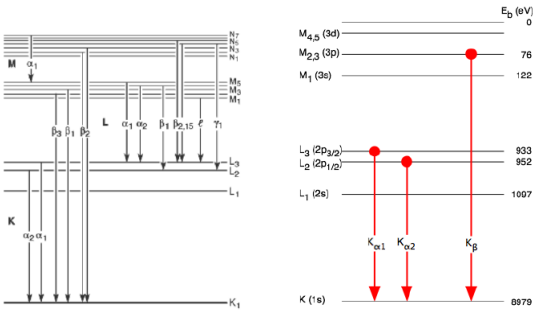

Figure 1.1: *Atomic levels involved in the X-ray emission according to the accepted terminology (line $K_{\alpha 1}$ corresponds to a transition from the $L_3(2p_{3/2})$ to the K (1s) level).*

When the emission lines are overlapped and/or the concentration of one of the elements is very low, the identification of the presence of a selected atomic species may not be possible and further inspections may be needed.

1.2 X-ray powder diffraction

In general, powder diffraction data are unsuitable for solving crystal structures. It is very difficult to be sure that the unit cell is correct as the reflections overlap and are difficult to resolve one from another. Crystallites smaller than ~120 nm create broadening of diffraction peaks.[2] This peak broadening can be used to quantify the average crystallite size of nanoparticles using the Scherrer equation

$$B(2\theta) = \frac{K\lambda}{L\cos(\theta)} \tag{1}$$

where $B(2\theta)$ is the peak length expressed in radians and computed as full width at half maximum of the powder diffraction peak. In the Gauss approximation the same FWHM instead of the same area can be considered, and the constant number $K = 0.94$ is used. The contribution of the peak width from the instrument by using a calibration curve must be known. Microstain may also create peak broadening. Analysing the peak widths over a long range of 2θ using a Williamson-Hull plot can let us separate microstain and crystallite size. L is the particle size.[4]

1.3 Raman spectroscopy

In addition to being absorbed and emitted by atoms and molecules, photons may also be scattered (approx. 1 in 10^7 in a transparent medium). This is due to a molecular effect which provides another way of studying of energy levels.

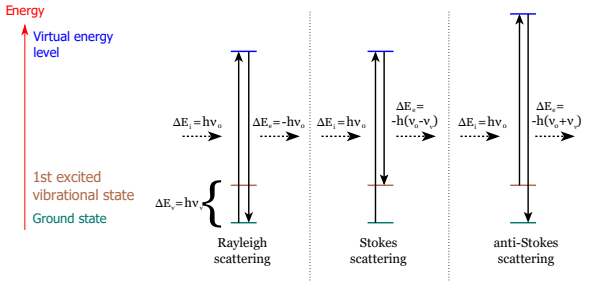

Figure 1.2: *The different possibilities of light scattering: Rayleigh scattering (no exchange of energy: incident and scattered photons have the same energy), Stokes Raman scattering (atom or molecule absorbs energy: scattered photon has less energy than the incident photon) and anti-Stokes Raman scattering (atom or molecule loses energy: scattered photon has more energy than the incident photon)*

The scattering may be: elastic and leave the molecule in the same state (Raylieigh Scattering) or inelastic and leave the molecule in a different quantum state (Raman Scattering). A material or molecule scatters irradiant light from a source and most of the scattered light is at the same wavelength as the laser source, but a small amount of light is scattered at different wavelengths. Not every crystal lattice vibration can be probed by Raman scattering. There are certain selection rules: Energy conservation: $\hbar\omega_i = \hbar\omega_s \pm \hbar\Omega$; where $\hbar\Omega$ is excitation energy, and momentum conservation in crystals $\mathbf{k_i} = \mathbf{k_s} \pm \mathbf{q} \Rightarrow 0 \leq |\mathbf{q}| \leq |\mathbf{k}| \Rightarrow 0 \leq |\mathbf{q}| \leq 4\pi n/\lambda_i$. Typically, in Raman spectroscopy high intensity laser radiation with wavelengths in either the visible or near-infrared regions of the spectrum is passed through a sample. Photons from the laser beam produce an oscillating polarization in the molecules, exciting them to a virtual energy state.

The oscillating polarization of the molecule can couple with other possible polarisations of the molecule, including vibrational and electronic excitation. Raman spectrum shows the intensity of the scattered light as a function of its frequency difference $\Delta\nu$ to the incident photons. The locations of corresponding Stokes and anti-Stokes peaks form a symmetric pattern around $\Delta\nu$=0. As seen on the figure 1.2 the frequency shifts are symmetric because they correspond to the energy difference between the same upper and lower resonant states. The intensities of the pairs of features will typically differ, though. They depend on the populations of the initial states of the material, which in turn depend on the temperature. In thermodynamic equilibrium, the upper state will be less populated than the lower state. Therefore, the rate of transitions from the lower to the upper state (Stokes transitions) will be higher than in the opposite direction (anti-Stokes transitions). Correspondingly, Stokes scattering peaks are stronger than anti-Stokes scattering peaks. Their ratio depends on the temperature (which can practically be exploited for the measurement of temperature).[3]

2 XRF of the unknown samples

2.1 Experimental setup

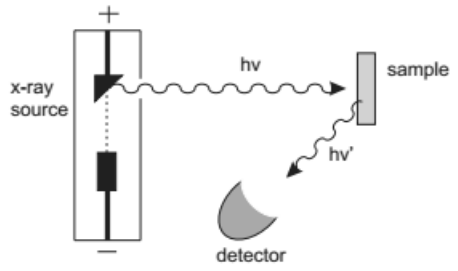

Figure 2.1: *XRF experimental setup*

The characteristic X-ray emission is induced by X-ray photons generator. The Coolidge tube is used in this experiment. In the Coolidge tube, the electrons are produced by thermionic effect from a tungsten filament (the cathode of the tube) heated by an electric current of 15 mA. The high voltage potential is between the cathode and the anode (which is made out of Mo), and the electrons are thus accelerated, and producing the X-rays while hitting the anode and bremsstrahlung while decelerating. The XRF technique here discussed is based on the primary excitation of a X-ray beam, followed by the secondary X-ray fluorescence emission (figure 2.1). A white beam generator which does not select a fixed wavelength is used. The beams of X-ray photons hit the sample perpendicularly and then the X-ray emission is detected and analysed by a photon detector (at the angle of 45° with respect to the incident beam), a Si solid state device characterized by a sufficient energy resolution. The samples do not need any specific preparation because the energy of the exciting photons is high enough (40 keV) allowing us to analyse depths of the order of 10 microns or more. [1]

2.2 Results and discussion

In this experiment qualitative analysis of unknown samples are performed only. For calibrating the system the equation $y = -0.118640 + 0.016568x$ is used. The goal of this particular calibration is to adjust each channel to corresponding energy given in keV. In the equation above variable x stands for the serial number of the multichannel analyser. Thus, calibration is done by the standard sample of known energy spectra. Then, the unknown elements are detected by reading and comparing the peaks of their spectra to the values available on the NIST government database in section specially dedicated for X-ray transitions [5]. As seen on figure 2.2 on the first unknown sample the Sb (L_α) Ga (K_α) and Ga (K_β) peaks are detected. The second sample provides us with more peaks including Ge (K_α and K_β transitions), Se (K_α and K_β transitions), Fe K_α and Ni (K edge). Peak which center is at approximately 11.1 keV is actually consisted of two separate peaks (Ge K_β and Se K_α) which are very close when this type of resolution system is used. On both graphs at the energies around 17 keV there are two peaks that correspond to Mo ($K_{\alpha 1}$ and $K_{\alpha 2}$) which is situated in the Coolidge tube as the anode that produces inci-

dent beams of X-rays which are used for generating XRF. The elastic scattering can be seen as well.

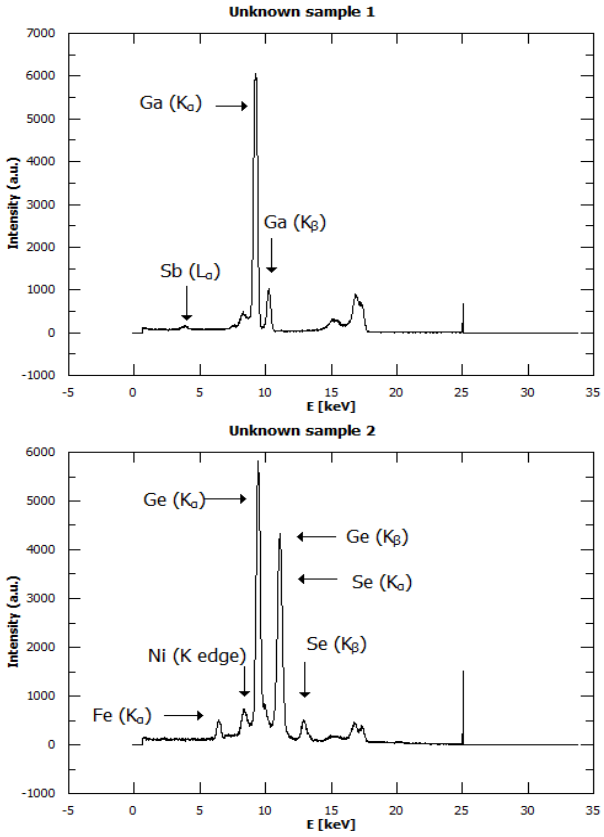

Figure 2.2: *The spectra of the unknown samples*

3 Powder diffraction of bulk and nano Bismuth crystal

3.1 Experimental setup

Essential parts of the diffractometer (figure 3.1) are: X-ray tube; the source of X-rays similar to the one used in XRF experiment, the goniometer; the platform that holds and moves the detector, the sample and the sample holder, receiving-side optics which conditions the X-ray beam after it has encountered the sample, and detector which counts the number of X-rays scattered by the sample.[2]

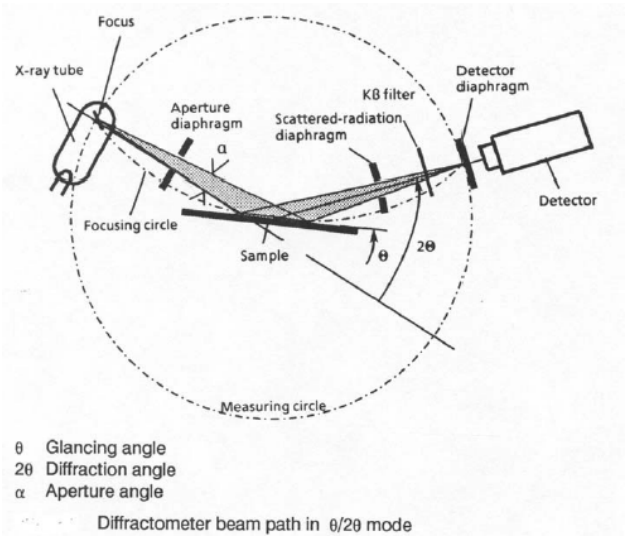

Figure 3.1: *XRD experimental setup*

An ideal powder sample should have many crystallites in random orientations. The distribution of orientations should be smooth and equally distributed amongst all orientations. If the crystallites in a sample are very large, there will not be a smooth distribution of crystal orientations. It will not provide a powder average diffraction pattern. Grains should be less than 10 microns in size to get good powder statistics. In order to get satisfying diffraction pattern in this experiment, a Bismuth powder was gathered on a thin capillary which was calibrated on a microscope with circular counter to put the capillary perpendicular to the incident X-rays.

3.2 Results and discussion

In this experiment, diffraction spectra of the nano and bulk Bi crystal were obtained. Data acquisition for Bi nano lasted for 8 hours, while for Bi bulk lasted for 1h 36 min. Fitting procedure was performed in the program Fityk. Black dots represent the plot of the data, blue lines represent Gaussian fits for the individual peaks, while red curve represents the overall fit on figure 3.2.

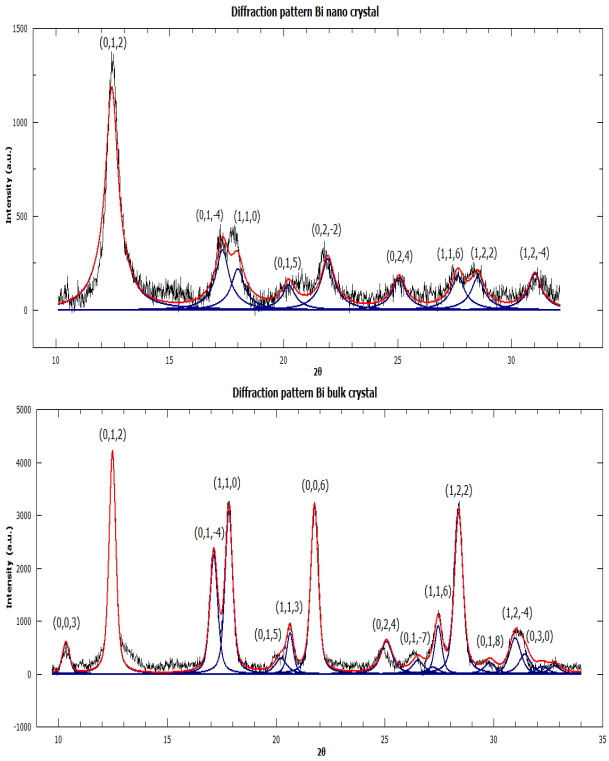

Figure 3.2: *The diffraction spectra of nano and bulk Bi crystals with Miller indices*

Sample	Particle size (nm)	Standard deviation (nm)
Bi nano crystal	5.378	± 0.056

Table 1: *Results of the crystallite size in the Bi nano sample*

After finding FWHM of each peak (blue curves) and computing mean values, the particle size of Bi nano crystal is determined using the equation (1). The results are given in the table 1. From the Bi bulk crystal pattern it is very difficult to determine the particle size, because bulk particles are too large to be easily detected by using XRD method and powder statistics.

4 Resolution Test of Micro Raman System

4.1 Experimental setup

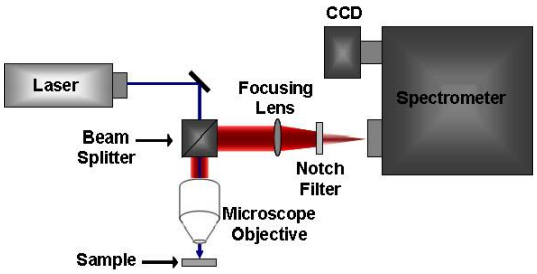

Figure 4.1: *Simple schematic diagram of Micro Raman system*

A Raman Micro-spectrometer (figure 4.1) consists of a specially designed Raman spectrometer integrated with an optical microscope. This allows the experimenter to acquire Raman spectra of microscopic samples or microscopic areas of larger samples. The advantages are that much less samples are required and certain effects may also be enhanced over very localized regions. In this experiment, the Micro Raman of the School of Science and Technology is used: 633 nm laser sources, fiber optics, Olympus microscope (up to 100x) with typical laser spot of 2-5 microns, Horiba iHR320 spectrometer with 2 gratings 1800/600 and Sincerity CCD, mapping XY (micrometer resolution). Furthermore, thin Si film is used as a sample (usually with Raman shift around 520 cm^{-1}). [3]

4.2 Results and discussion

Each set of data is scanned 10 times, where each period of scan lasted for 30s. In the experiment we give a description about the change in the resolution when different grating number (GN) and magnification (MG) is used.

Features	Center (cm^{-1})	FWHM (cm^{-1})	Height (counts)	Area
1800_x50_30s_10t	519.36	5.48	8668	50514
	512.81	9.32	2676	26547
1800_x5_30s_10t	519.81	5.23	172	968
	512.81	8.29	55	489
600_x50_30s_10t	519.83	12.84	32042	437837
	512.81	18.35	4604	89907
600_x5_30s_10t	519.83	12.10	496	6389
	512.81	17.39	79	1460

Table 2: *Gaussian Peak parameters of the blue curves represented in figure 4.2 for different setup features*

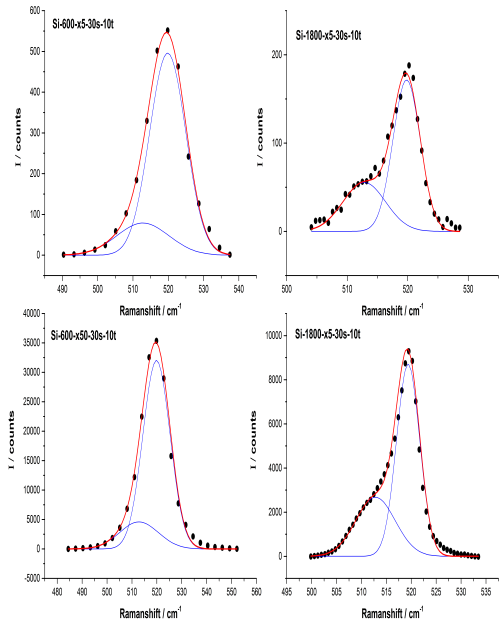

Figure 4.2: *In this figure, the dots are the plot of the data; the red curve is the best fit of the data; the two blue Gaussian peaks are the separate peaks that consists the red curve*

As it is known the FWHM of the fitted curve of the acquired data can be a measure of the resolution of the system (with unit cm^{-1}/pixel). The lower the value of FWHM, the better the resolution and the better two closely placed objects can be differentiated or separated. For the intensity, we wish we could collect more photons scattered from the sample to have clearer image. In this data file we get four sets of data, for each of which we have modified the GN (between 1800 g/mm and 600 g/mm) and the magnification (between x50 and x5). The consequence of the modification is obvious to reflect the change on the resolution and the peak intensity.

Hence we made a comparison by plotting the data and fitting by two Gaussian Peaks with different parameters as shown in the figure 4.2 and table 2. It is decided to have two Gaussian fitting peaks for each set of data. It can be seen from the graph of the 4th red curve (1800 g/mm x50) in figure 4.2 that there are two peaks located at 512.8 cm^{-1} and 519.4 cm^{-1}.It is assumed each fitting should consists of two peaks approximately at 513 cm^{-1} and 520 cm^{-1}.

By the data at hand, we observed that:

1. The most obvious change is in FWHM and peak intensity. As GN changes from 600 g/mm to 1800 g/mm, the resolution improves about twice. From table 2, for the peaks centered at 519.8 with magnification x50, FWHM is 12.84 cm^{-1} for 600 g/mm while it is 5.48 cm^{-1} for 1800 g/mm.

2. As GN changes from 600 g/mm to 1800 g/mm, the peak intensity drops dramatically. From table 2, with the same magnification of x50, the peak for 600 g/mm reached 32042 counts, whereas it is 8668 counts for 1800 g/mm.

3. MG changes from x5 to x50, peak intensity will increase dramatically. For example, with fixed 1800 g/mm, 8668 counts are acquired for x50 and 172 counts for x5.

4. As MG changes from x5 to x50, our resolution will drop.

5 Conclusions

Using XRF qualitative analysis the elements in the unknown samples are determined. It is found that in the first unknown sample, the Ga lines with Sb were present, while in the second unknown sample Ge, Ni, Se and Fe lines were detected.

In the second experiment the crystallite size of nano Bismuth crystal was computed. It was achieved by using XRD pattern, measuring and averaging FWHM of diffraction spectra peaks and by using Scherrer equation. Particle size of Bi nano crystal equals 5.378 ± 0.056 nm.

By doing resolution test of Micro Raman system it is observed that grating number is of an important influence on the resolution of the system (which is connected with peak's FWHM). Greater the GN, smaller the FWHM which implies better resolution.

References

[1] Andrea di Cicco, Lectures about XRF (X-Ray Flourescence), Advanced Physics Laboratory, Laurea Magistrale in Fisica, University of Camerino, 2013

[2] Scott A. Speakman, Patrick McArdle (Edited by Di Cicco), An Introduction to X-Ray Powder Diffraction, University of Camerino, 2014

[3] A. Sirenko, R. Horn (Edited by Di Cicco), An Introduction to optical Raman Scattering, University of Camerino, 2016

[4] Fabio Iesari, Diffrazione dei raggi X su materiali nanocristallini: studio del Bismutho (Tesi di Laurea Triennale), University of Camerino, 2010

[5] NIST X-ray Transition Energies Database http://physics.nist.gov/PhysRefData/XrayTrans/Html/search.html